PHYSICAL REVIEW B **73**, 140406(R) (2006)

Magnetic-field and pressure dependence of low-temperature resistivity in UGe_2

T. Terashima, K. Enomoto, T. Konoike, T. Matsumoto, and S. Uji
National Institute for Materials Science, Tsukuba, Ibaraki 305-0003, Japan

N. Kimura, M. Endo, T. Komatsubara, and H. Aoki
Center for Low Temperature Science, Tohoku University, Sendai, Miyagi 980-8578, Japan

K. Maezawa
Department of Liberal Arts and Sciences, Toyama Prefectural University, Kosugi, Toyama 939-0398, Japan
(Received 28 February 2006; published 25 April 2006)

We report measurements of resistivity ρ in UGe_2 at temperatures T down to 0.3 K, pressures P up to 19.8 kbar, and magnetic fields B_{appl} up to 17.5 T applied along the magnetic easy a axis. The coefficient A of the T^2 term of $\rho(T)$ is determined as a function of B_{appl} and P. In the large-moment ferromagnetic phase (the low-P/high-B_{appl} phase), A is found to be a function of the single parameter $(B_{appl}-B_x)$ and approximately obeys a power law $A \propto (B_{appl}-B_x)^{-1/2}$, where B_x is the transition field from the small- to the large-moment ferromagnetic phase. The T dependence of ρ at fields just above B_x suggests a contribution to ρ from excitations with a gapped spectrum.

DOI: 10.1103/PhysRevB.73.140406 PACS number(s): 75.30.Kz, 74.70.Tx, 71.27.+a, 72.15.Eb

The discovery of superconductivity (SC) in the itinerant-electron ferromagnet UGe_2 has caused much excitement.[1] It was almost clear from the beginning that an early concept of ferromagnetic (FM)-spin-fluctuation-mediated SC is not directly applicable. Contrary to the expectation that this type of SC appears on either side of a FM-paramagnetic (PM) boundary,[2] the SC in UGe_2 is observed only in FM phases. Although some theoretical ideas have been proposed,[3–5] the mechanism of this peculiar SC remains to be unraveled.

The Curie temperature T_C of UGe_2 is 52 K at ambient pressure,[6] gradually decreases with pressure P, and finally collapses to zero at the critical pressure P_c (~16 kbar) [see the inset of Fig. 1(c)].[1,7–9] The transition is first order near P_c (Refs. 10–12). Above P_c, as the magnetic field B_{appl} is applied along the magnetic easy a axis,[13] a metamagnetic transition from a PM to a FM phase occurs at the transition field B_m (Ref. 10). There is another phase transition (or a crossover at low P) at the temperature T_x inside the FM phase[14]: the magnetization sharply increases below T_x (Refs. 8 and 15). T_x is ~30 K at ambient P, decreases with P, and appears to reach zero at another critical pressure P_x (~12–13 kbar).[8,9,14] There is a debate about the order of the transition near P_x (Refs. 12 and 16). Above P_x, the T_x transition can be induced at the transition field B_x (Refs. 8 and 15). We hereafter call the two FM phases the small-moment [***S*** in the inset of Fig. 1(c)] and the large-moment FM phase (***L***), respectively. Magnetic properties of UGe_2 are extremely anisotropic with an anisotropy field of the order of 100 T (Ref. 13), and no field-induced transition occurs for field directions perpendicular to the a axis. The SC is observed in a P range ~10–16 kbar, and the maximum transition temperature (T_{SC}~0.8 K) is found near P_x (Refs. 1, 8, and 9). The electronic specific-heat coefficient γ, quasiparticle mass m^*, and the coefficient A of the T^2 term of resistivity ρ (i.e., $\rho=\rho_o+AT^2$) peak near P_x or rise steeply across P_x (Refs. 8, 9, and 11). These observations have led to theoretical scenarios relating the T_x transition and the SC (Refs. 4 and 5).

In this paper, we report measurements of low-T resistivity in UGe_2 in a wide range of P and B_{appl}. We show that, as the small-moment FM phase is approached from the large-moment FM phase, A is enhanced in a peculiar manner and that an extra contribution to $\rho(T)$ other than the T^2 term appears.

The single-crystalline specimen used in this study was cut from a UGe_2 ingot grown by the Czochralski pulling method. The residual resistivity ratio is 96. A conventional ac four-terminal method was used with an electrical current (f =11 Hz, $I \leq 300$ μA) along the a axis. The magnetic field B_{appl} up to 17.5 T was also applied along the a axis. Hydrostatic pressures P up to 19.8 kbar were produced by a BeCu/NiCrAl clamped piston-cylinder cell with a 1:1 mixture of 1-propanol and 2-propanol as a pressure-transmitting medium.[11,17] The pressure was measured with a manganin gauge calibrated against the superconducting transition of tin. Low temperatures down to 0.3 K were achieved with a ^{3}He refrigerator. The temperature was measured with a RuO_2 resistance thermometer, which was calibrated in fields up to 17.5 T below 4.2 K and at zero field up to 10 K.

We first determine the P-B_{appl} phase diagram. ρ versus B_{appl} curves are most conveniently used to locate B_x and B_m, as exemplified in Fig. 1(a) for P=14.8 kbar. These ρ versus B_{appl} curves are similar to previously reported ones.[18] The transition at B_m is characterized by a steep rise in ρ, while that at B_x manifests itself as a bend. To avoid ambiguity, we adopt the following practical definitions: B_x and B_m are determined by the position of a negative peak of $d^2\rho/dB_{appl}^2$ and that of a positive peak of $d\rho/dB_{appl}$, respectively. No hysteresis is observed either at B_x or at B_m. Neither B_x nor B_m exhibits appreciable T dependence in the investigated T range. Figure 1(b) shows ρ versus T curves measured at two pressures near P_x. The curve at 11.1 kbar shows a kink near 7 K, a characteristic of the T_x anomaly,[8,9,14] while that at

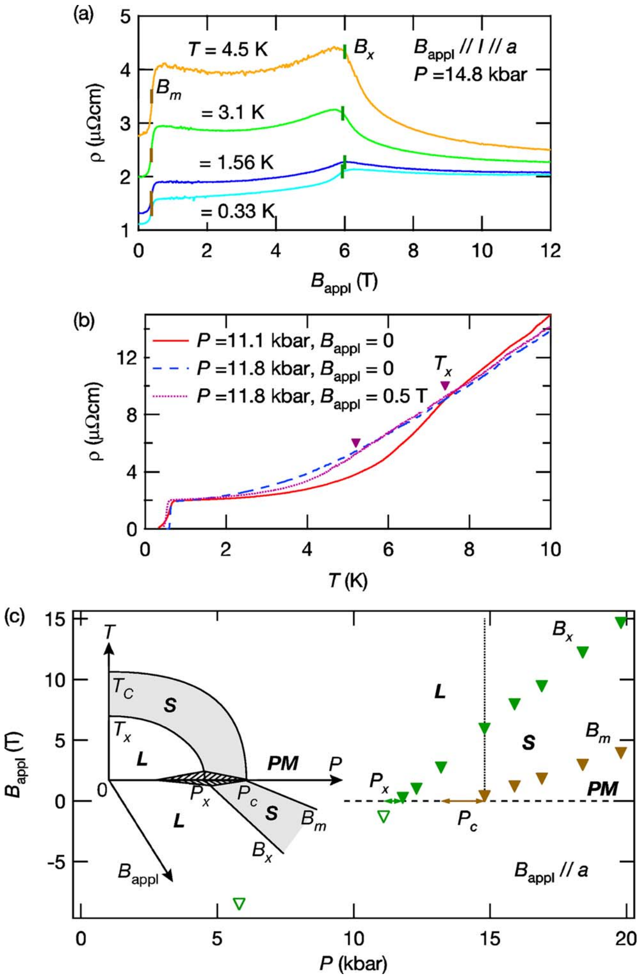

FIG. 1. (Color online) (a) ρ vs B_{appl} curves at $P=14.8$ kbar. The transition fields B_x and B_m are marked. (b) Examples of ρ vs T curves. The T_x anomalies observed at $(P,B_{appl})=(11.1\text{ kbar},0\text{ T})$ and $(11.8\text{ kbar},0.5\text{ T})$ are marked. (c) P-B_{appl} phase diagram showing B_x and B_m. For the two negative values of B_x (open symbols), see text. P_x and P_c are estimated to be in the P regions denoted by the horizontal lines with arrows. The symbols ***L***, ***S***, and ***PM*** denote the large-moment FM, the small-moment FM, and the paramagnetic phase, respectively. The vertical dotted line at $P=14.8$ kbar indicates the line along which the data in Fig. 2(b) were collected. The inset shows a schematic P-B_{appl}-T phase diagram. The SC occurs in the hatched area.

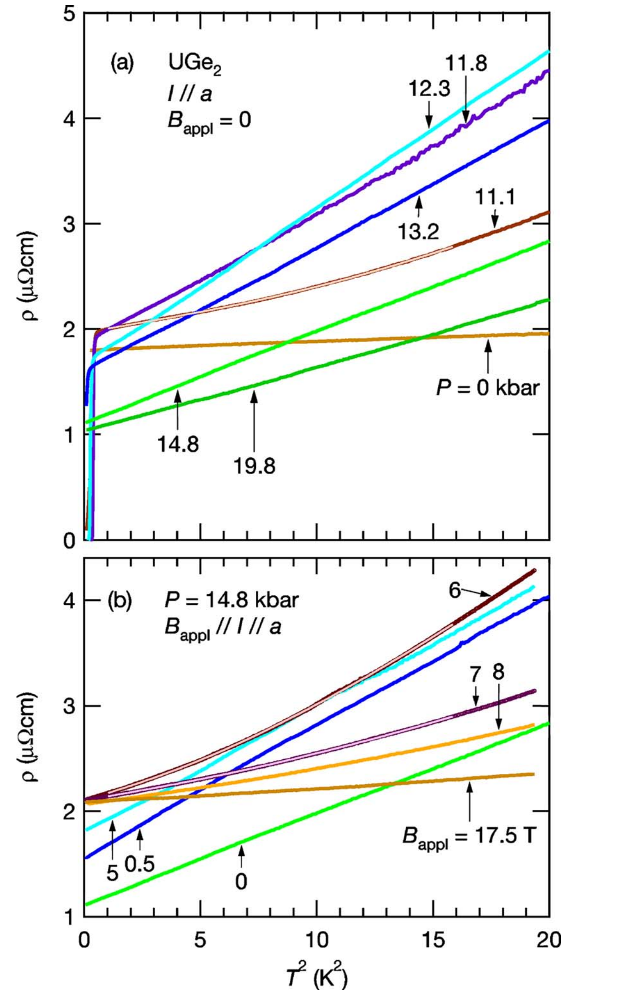

FIG. 2. (Color online) Selected ρ vs T^2 curves (a) at zero field for various P's and (b) at 14.8 kbar for various B_{appl}'s. For $P=11.1$ kbar in (a) and $B_{appl}=6$ and 7 T in (b), the fits of Eq. (1) to the data in the T range $1\text{ K}<T<4$ K are also shown in pale colors and are almost indistinguishable from the data.

11.8 kbar ($B_{appl}=0$) does not. This indicates $11.1\text{ kbar}<P_x<11.8$ kbar. A field of 0.5 T revives a kink near 5 K, indicating $0<B_x<0.5$ T at $P=11.8$ kbar.

Figure 1(c) shows the determined phase diagram (the two negative values of B_x are explained below). We have used ρ versus B_{appl} curves at $T=0.3$ K for most pressures. The exceptions are 11.8 and 12.3 kbar, where the B_x transitions at 0.3 K are masked by the SC; B_x at 12.3 kbar is determined from a ρ versus B_{appl} curve at 0.8 K, while B_x at 11.8 kbar is estimated to be 0.25 (±0.25) T from the two ρ versus T curves mentioned above. The present phase diagram is qualitatively consistent with those previously reported[12,19,20]: Both transition fields increase nearly linearly with P, B_x having a larger slope. However, we note that the values of the critical fields/pressures differ considerably among various reports.[10,12,18] To demonstrate the sample dependence, we compare the ratio B_x/B_m for a given B_x, which ratio is free from possible error in pressure determination: the ratios at $B_x\sim 7$ T, for example, are 8.7, 4.9, and 3.6 for the present data and Refs. 12 and 18, respectively.

We next examine the evolution of ρ with P and B_{appl}. Figure 2(a) shows ρ as a function of T^2 at zero field for various P's. At ambient P, the sample is in the large-moment FM phase, and the ρ versus T^2 curve is straight with a small slope, i.e., a small A. As P is increased towards P_x, T_x decreases and approaches the highest T (~4.5 K) of Fig. 2. The nearby T_x transition gives rise to a curvature in the ρ versus T^2 curve ($P=11.1$ kbar). The curve, however, asymptotically approaches a straight line as $T\rightarrow 0$, and A in the limit of $T\rightarrow 0$ is larger than at ambient P. As the sample enters the small-moment FM phase at 11.8 kbar, the ρ versus T^2 curve becomes straight again, and A is substantially enhanced. The ρ versus T^2 curve does not vary very much with P in the small-moment FM phase (P up to 13.2 kbar). As the sample enters the PM phase at 14.8 kbar, the residual resistivity decreases abruptly. As previously noted,[8] the T^2 dependence of ρ is retained even near P_c, which is consistent with the first-order transition near P_c. A gradually decreases with P in the PM phase, though it is still much larger at 19.8 kbar than at ambient P. For the SC, an incipient resistivity drop can already be detected at 5.8 kbar. The zero resistivity is, however, observed only above P_x, at 11.8 and 12.3 kbar. T_{SC} and the upper critical field at $T=0.4$ K are 0.62 K and $\sim$1 T for 11.8 kbar, and 0.52 K and 1.2 T for 12.3 kbar. While the onset of the SC can still be seen at 13.2 kbar, no indication of the SC is found at 14.8 kbar ($>P_c$): i.e., it is confirmed that the disappearance of the SC coincides with P_c.

Figure 2(b) illustrates the influence of B_{appl} at 14.8 kbar. As can be seen from Fig. 1(c), decreasing B_{appl} at 14.8 kbar (see the vertical dotted line at $P=14.8$ kbar) is equivalent to increasing P at zero field in the sense that the phases appear successively in the same order. Thus we view the curves in Fig. 2(b) in descending order of B_{appl}; the sample is in the large-moment FM phase from $B_{appl}=17.5$ down to 6 T, in the small-moment FM phase from 5 down to 0.5 T, and in the PM phase at 0 T. It is apparent that Figs. 2(a) and 2(b) are analogous with each other.

We now look at the extra contribution to ρ, other than the usual electron-electron scattering T^2 term in a Fermi liquid, found in the large-moment FM phase near P_x or B_x. We can achieve excellent fits to the 11.1-kbar (just below P_x) data in Fig. 2(a) and to the 6- and 7-T data at 14.8 kbar, where $B_x=5.9$ T, in Fig. 2(b) in the T range 1 K$<T<$4 K, by using the following expression[21]:

$$\rho = \rho_o + AT^2 + b(T/\Delta)(1 + 2T/\Delta)\exp(-\Delta/T). \qquad (1)$$

The estimated values of Δ are 17 K for the 11.1-kbar data and 10 and 13 K for $B_{appl}=6$ and 7 T, respectively. For other pressures ($>P_x$), fits to data measured just above B_x yield Δ's of 10–20 K. We note that, since the contribution of the last term diminishes rapidly as B_{appl} is increased from B_x, meaningful fits can only be done just above B_x.

The last term of Eq. (1) was originally derived for electron-magnon scattering in a metallic local-moment ferromagnet with a magnon energy gap Δ (Ref. 21). However, since UGe_2 is an itinerant-electron ferromagnet, we would need a different interpretation of this term. Indeed, the above estimated Δ would be too small for an anisotropy gap in UGe_2 with the large anisotropy field. Interestingly, Aso *et al.* have recently suggested the existence of a gap in the magnetic excitation spectrum of UGe_2 from the analysis of the T dependence of spontaneous magnetization.[22] The gap is estimated at $\sim$10 K just below P_x, which is similar in size to our gap. However, Aso *et al.* identify it with a Stoner gap, and its relation to our gap is not clear.

We basically determine the coefficient A by fitting a straight line to ρ versus T^2 curves in the range 1 K$^2<T^2<$5 K^2, except just above B_x, where Eq. (1) is used as described above. However, we note that the last term of Eq. (1) is actually not so influential in estimating A, since it is exponentially small at low T; the difference between A values determined by the two methods is $\sim$10% at most. The resultant A is shown in Fig. 3.

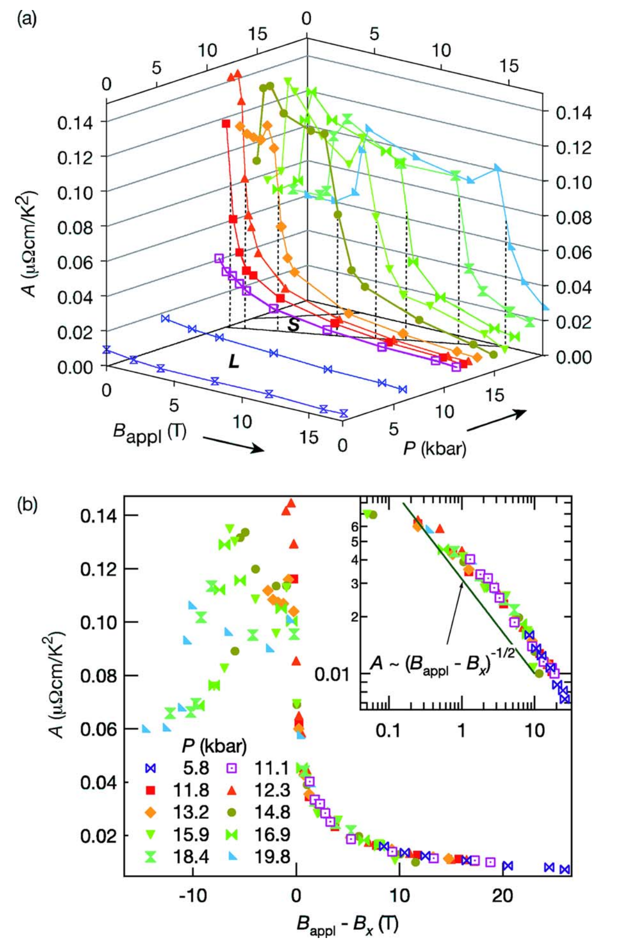

FIG. 3. (Color online) (a) The coefficient A of the T^2 term of ρ as a function of B_{appl} for various P's. The vertical broken lines indicate the positions of B_x. The two lines on the B_{appl} - P plane indicate B_x and B_m, and ***L*** and ***S*** denote the large-moment and the small-moment FM phase, respectively. (b) The same data as (a) except the $P=0$ kbar data are plotted as a function of $B_{appl}-B_x$. For $P=5.8$ and 11.1 kbar, the negative values of B_x shown in Fig. 1(c) are used. A log-log plot (inset) suggests a power-law behavior for $B_{appl}-B_x>0$.

The obtained P dependence of A at zero field is very similar to that reported by Kobayashi *et al.*[18] except the following: (1) The present values are about 60% larger. (2) Kobayashi *et al.* observed a plateau of A between P_x and P_c, which is not clear in our data since we have only three data points in the region. The present zero-field data can also be compared with γ, which was measured up to P_c by Tateiwa *et al.*[9,23] The proportionality between $\sqrt{A}$ and γ is obeyed better than ±20%, and the average ratio of A/γ^2 is consistent with the universal value of $\sim 1\times10^{-5}$ $\mu\Omega$ cm(mol K/mJ)^2 (Ref. 24). Tateiwa *et al.* also determined γ in magnetic fields at 12.8 kbar (Ref. 16). The comparison between γ at (P, B_{appl})=(12.8 kbar, 7 T) and A at (12.3 kbar, 8 T) or (13.2 kbar, 8 T) suggests that the proportionality holds in magnetic fields.

We now focus on the region $P<P_x$. Since no field-induced transition occurs in this region, we may compare experimental observations with conventional theories of spin

fluctuations. We then find that neither the P nor the field dependence of A in UGe_2 conforms to theoretical predictions. First, the expected relation[25] $A \propto M_s^{-1}$, where M_s is the spontaneous magnetization at absolute zero, is not observed: on going from 0 to 11.1 kbar, just below P_x, A at zero field increases by a factor of 4, while M_s decreases by only 10% (Ref. 12). Secondly, the field dependence of A is too large. A is reduced by ~50% (0 and 5.8 kbar) or ~75% (11.1 kbar) at 17.5 T, while a theoretical model[26] predicts only ~20% reduction.[29]

We now turn to the field dependence of A above B_x in the region $P > P_x$. The A versus B_{appl} curves above B_x (i.e., in the large-moment FM phase) for different P's look very similar [Fig. 3(a)]. We therefore replot A in the region $P > P_x$ as a function of $B_{appl} - B_x$ [solid symbols in Fig. 3(b)] and find that all the data points lie on a single universal curve for $B_{appl} - B_x > 0$. Furthermore, we find that data points at 5.8 and 11.1 kbar, which are below P_x, also follow the same curve by using appropriate negative values for B_x [open symbols in Fig. 3(b)]. These negative "B_x's" are shown in Fig. 1(c) with open symbols. We have omitted the ambient-P data since the estimation of B_x is so ambiguous. The inset of Fig. 3(b) indicates that A varies as $(B_{appl} - B_x)^{-1/2}$ except for the rounding in the immediate vicinity of B_x. We also note that A actually peaks slightly below B_x [see Fig. 3(a)]. The following may partly account for these deviations from the power law: (1) The true transition field might be smaller than B_x determined by the present definition. (2) P distribution causes distribution of B_x in the sample: note only 0.1 kbar difference in P results in ~0.2 T difference in B_x [see Fig. 1(c)]. It is difficult to tell the true behavior of A in the limit of $B_{appl} \rightarrow B_x$, i.e., whether it diverges or not. For $B_{appl} - B_x < 0$, no universal behavior is observed. This may be due to the influence of B_m. It seems that A in the small-moment FM phase is the sum of two contributions peaking near B_m and B_x. We also note that plotting A against $B_{appl} - B_m$ does not reveal any universal behavior.

We may recall that spin-fluctuation theories suggest $A \propto S^{1/2}$, where S is the Stoner enhancement factor and diverges at a FM-PM boundary.[25] However, it seems difficult to relate the observed power law to this theoretical prediction, since B_x is not a FM-PM boundary.

Power-law dependence of A on magnetic field is reported for $CeNi_2Ge_2$ and $YbRh_2Si_2$, for example: $A \propto B^{-0.6}$ for the former,[27] and $A \propto (B - B_c)^{-1}$ for the latter,[28] where B_c is a metamagnetic transition field. Both compounds exhibit pronounced non-Fermi-liquid behavior in thermodynamic, magnetic, and transport properties as $B \rightarrow 0$ or B_c, and the power laws are discussed in terms of quantum critical spin fluctuations.[27,28] In the case of UGe_2, however, there has been no report of non-Fermi-liquid behavior in the vicinity of B_x.

Irrespective of whether P is below P_x or above P_x, A in the large-moment FM phase is determined by the single parameter $B_{appl} - B_x$ at each P, and B_x varies from negative to positive approximately linearly with P across P_x. These may be favorable to theoretical scenarios assuming a characteristic energy (level) ϵ_x in the electronic structure and that the T_x transition occurs when the Fermi level ϵ_F equals ϵ_x (Refs. 5 and 12). Various physical properties would then be governed by the distance $\epsilon_x - \epsilon_F$ in the majority-spin band, which distance in first approximation would shift linearly with B_{appl} or P. Our experimental findings provide a crucial test for such scenarios, that is, whether they can reproduce the power law of A observed only in the large-moment FM phase. In addition, the origin of the gapped excitations suggested by $\rho(T)$ at fields just above B_x has to be accounted for.

We thank K. Tanaka and M. Nishimura for technical assistance. This work was supported by Grants-in-Aid for Scientific Research from the JSPS, Japan.

[1] S. S. Saxena *et al.*, Nature (London) **406**, 587 (2000).
[2] D. Fay and J. Appel, Phys. Rev. B **22**, 3173 (1980).
[3] H. Suhl, Phys. Rev. Lett. **87**, 167007 (2001).
[4] S. Watanabe and K. Miyake, J. Phys. Soc. Jpn. **71**, 2489 (2002).
[5] K. G. Sandeman *et al.*, Phys. Rev. Lett. **90**, 167005 (2003).
[6] C. E. Olsen, J. Appl. Phys. **31**, S340 (1960).
[7] H. Takahashi *et al.*, Physica B **186–188**, 772 (1993).
[8] A. Huxley *et al.*, Phys. Rev. B **63**, 144519 (2001).
[9] N. Tateiwa *et al.*, J. Phys.: Condens. Matter **13**, L17 (2001).
[10] A. Huxley *et al.*, Physica B **284–288**, 1277 (2000).
[11] T. Terashima *et al.*, Phys. Rev. Lett. **87**, 166401 (2001).
[12] C. Pfleiderer and A. D. Huxley, Phys. Rev. Lett. **89**, 147005 (2002).
[13] A. Menovsky *et al.*, in *High Field Magnetism*, edited by M. Date (North-Holland, Amsterdam, 1983).
[14] G. Oomi *et al.*, Physica B **206 & 207**, 515 (1995).
[15] N. Tateiwa *et al.*, J. Phys. Soc. Jpn. **70**, 2876 (2001).
[16] N. Tateiwa *et al.*, Phys. Rev. B **69**, 180513(R) (2004).
[17] M. Endo *et al.*, Phys. Rev. Lett. **93**, 247003 (2004).
[18] T. C. Kobayashi *et al.*, J. Phys.: Condens. Matter **14**, 10779 (2002).
[19] T. Terashima *et al.*, Phys. Rev. B **65**, 174501 (2002).
[20] Y. Haga *et al.*, J. Phys.: Condens. Matter **14**, L125 (2002).
[21] N. H. Andersen and H. Smith, Phys. Rev. B **19**, 384 (1979).
[22] N. Aso *et al.*, Phys. Rev. B **73**, 054512 (2006).
[23] N. Tateiwa *et al.*, Physica B **312–313**, 109 (2002).
[24] K. Kadowaki and S. B. Woods, Solid State Commun. **58**, 507 (1986).
[25] T. Moriya, *Spin Fluctuations in Itinerant Electron Magnetism* (Springer-Verlag, Berlin, 1985).
[26] K. Ueda, Solid State Commun. **19**, 965 (1976).
[27] P. Gegenwart *et al.*, Phys. Rev. Lett. **82**, 1293 (1999).
[28] P. Gegenwart *et al.*, Phys. Rev. Lett. **89**, 056402 (2002).
[29] We have used Eq. (6) of Ref. 26. Using magnetization curves in Ref. 12, the normalizing magnetic fields $L\zeta_0^3$ are estimated at 82.1, 111, and 73.4 T for 0, 5.8, and 11.1 kbar, respectively. The parameter $\tilde{L}$ is assumed to be 1–2 as usual.